Editors' Suggestion

Hanbury Brown–Twiss Correlations for a Driven Superatom

J. Lampen, A. Duspayev, H. Nguyen, H. Tamura, P. R. Berman, and A. Kuzmich
Department of Physics, University of Michigan, Ann Arbor, Michigan 48109, USA

(Received 10 September 2019; published 15 November 2019)

Hanbury Brown–Twiss interference and stimulated emission, two fundamental processes in atomic physics, have been studied in a wide range of applications in science and technology. We study interference effects that occur when a weak probe is sent through a gas of two-level atoms that are prepared in a singly excited collective (Dicke or "superatom") state and for atoms prepared in a factorized state. We measure the time-integrated second-order correlation function $g^{(2)}$ of the output field as a function of the delay τ between the input probe field and radiation emitted by the atoms and find that, for the Dicke state, $g^{(2)}$ is twice as large for $\tau = 0$ as it is for $\gamma_e \tau \gg 1$ (γ_e is an excited state decay rate), while for the product state, this ratio is equal to $3/2$. The results agree with those of a theoretical model in which any effects related to stimulated emission are totally neglected—the coincidence counts measured in our experiment arise from Hanbury Brown–Twiss interference between the input field and the field radiated by the atoms.

DOI: 10.1103/PhysRevLett.123.203603

In his 1917 paper [1], Einstein introduced his famous A and B coefficients, with the A coefficient associated with spontaneous emission and the B coefficient with either absorption or stimulated emission (both referred to as "changes of state due to irradiation" by Einstein). While there may not be a universal definition as to what constitutes stimulated emission, any definition describes processes in which atom-field interactions lead to an increase in the intensity of an input field. There have been a number of both theoretical analyses and experimental implementations involving parametric down-conversion (e.g., Refs. [2–7]), which have been interpreted in terms of stimulated emission and/or amplification. In all of these cases, coincidence counts involving both signal and idler modes are measured when a single-photon or a weak coherent probe pulse is sent into a crystal, so that it propagates collinearly with the signal mode. A twofold increase in the time-integrated coincidence counts occurs for overlapping probe and signal field pulses, compared to the case of nonoverlapping pulses. The increase in coincidence counts was interpreted in terms of probe-induced stimulated emission in the crystal. The analyses supporting this assertion are based on a perturbative calculation of the evolution of the state vector associated with an effective Hamiltonian involving third-order nonlinear susceptibilities.

We have carried out an experiment that, in some ways, is analogous to the down-conversion experiments. Instead of a nonlinear crystal, our active medium consists of a gas of cold rubidium atoms, Fig. 1(a). Following their release from an optical trap, the atoms are subjected to an excitation-deexcitation pulse sequence, leading to phase-matched emission in the x direction having central frequency ω_A. A weak probe pulse having central frequency ω_P is also sent into the sample in the x direction and can be delayed relative to the phase-matched emission pulse. The output field, containing contributions from both the input field and the field radiated by the atoms, is sent to a beam splitter and coincidence counts are recorded as a function of the delay time. As in the down-conversion experiments, we can observe an increase in coincidence counts by a factor of 2 when the probe field overlaps with the field radiated by the atoms.

What is the origin of this increase in coincidence counts? Can it be traced to stimulated emission as is claimed in down-conversion experiments, or are there other mechanisms at play here? To help answer these questions, we prepare our atomic ensemble in two distinct fashions, one involving a single excitation (superatom or Dicke [8] state) and the other a factorized initial state. We are able to do this by choosing different Rydberg states in the excitation schemes. The results are analyzed using source-field theory [9]. In the case of the Dicke state preparation, there is a single excitation shared by N atoms and the incoming probe pulse can drive a stimulated transition between the Dicke state and the ground state. The coupling strength between the two collective states is enhanced by a factor $\sqrt{N}$. As a consequence, one might associate the increased coincidence counts with stimulated emission. On the other hand, for a factorized initial atomic state, such an interpretation is no longer tenable since the incident probe field is actually absorbed by the medium. In both cases, however, an increase in coincidence counts is observed. We present experimental results and a theoretical analysis that leads us to conclude that stimulated emission is *not* responsible for the increase in coincidence counts. Instead, the increase in coincidence counts can be attributed to Hanbury Brown–Twiss (HBT) interference [10], which we

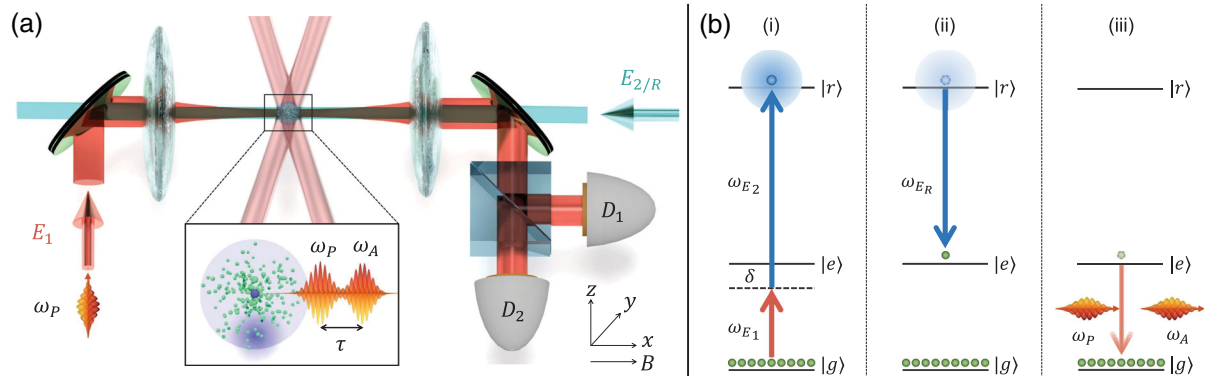

FIG. 1. Outline of the experiment. (a) Experimental setup: an ultracold atomic gas is prepared in a crossed pair of focused yttrium-aluminum-garnet laser beams. A pair of lenses focuses E_1 and E_2 laser fields to drive a two-photon transition from the ground state $|g\rangle$ to the Rydberg state $|r\rangle$. A retrieval laser pulse E_R leads to emission of an atomic field that is split on a beam splitter and directed onto photodetectors D_1 and D_2. A probe laser field with controllable frequency and delay is aligned into the spatial mode of the atomic emission. (b) Three main steps of the protocol: (i) an atomic ensemble is excited into a Rydberg atomic state $|r\rangle$; (ii) after a delay T_s, the atoms are driven into intermediate state $|e\rangle$, leading to emission on the $|e\rangle \leftrightarrow |g\rangle$ transition, with propagation direction determined by the phase-matching condition; (iii) an incoming probe field and atomic emission fields, with controllable delay between the two fields, are directed toward HBT measurement.

claim can also explain the increase in coincidence counts measured in the down-conversion experiments [11].

To illustrate the underlying physics, we consider first a single-photon probe pulse incident on a two-level atom (lower level g and excited level e) that is prepared in its excited state at time $t = 0$. The wave front of the probe pulse, which has cross-sectional area A greater than the square of the pulse's central wavelength λ, arrives at the atom at time $\tau \geq 0$. In source-field theory [12], the positive frequency component of the field operator for this system can be written as $E_+(\mathbf{R}, t) = E_+^{(0)}(\mathbf{R}, t) + E_+^{(S)}(\mathbf{R}, t)$, where $E_+^{(0)}(\mathbf{R}, t)$ is the free-field operator and $E_+^{(S)}(\mathbf{R}, t)$ is the source-field operator associated with the field radiated by the atoms in the sample. Two types of measurements can be envisioned. Either (1) the integrated field intensity is measured or (2) the time-integrated number of coincidence counts is recorded as a function of τ after the field is sent through a beam splitter. The detection volume is restricted to a small angle in the forward direction.

For $A \gg \lambda^2$, a "weak coupling" approximation can be made—the interaction between the atoms and the input pulse can be neglected to lowest order, owing to the fact that $\max[\Omega_p/\gamma_e \ll 1, \Omega_p T_p \ll 1]$, where Ω_p is the probe Rabi frequency, T_p is the probe pulse duration, and γ_e is the excited state decay rate. It is then rather easy to analyze the two measurement scenarios, which are sensitive to different physical processes. The total field can be viewed as a sum of the collimated input field, the spherical wave spontaneously emitted field from the atom, and the field scattered by the atom.

The integrated field intensity is sensitive to the *amplitudes* of the three contributions to the total field. Stimulated emission or absorption is associated with the interference of the scattered field with the (unperturbed) input field [13]. Whether stimulated emission or absorption occurs depends on both the spectral width of the input pulse and the time delay τ. In contrast, the time-integrated number of coincidence counts N_c is insensitive to the relative phase of the input and source fields—it depends only on field intensities. Moreover, in the weak coupling approximation, the scattered field has a negligible effect on the value of N_c. When measured as a function of τ, N_c exhibits a "bump" for $\tau = 0$ that can then be interpreted as HBT interference between the input field and the field spontaneously emitted from the atoms, in exact analogy with the HBT increase in the second-order correlation function for two independent light sources. In other words, although both stimulated emission and HBT interference can be described in terms of interference, they correspond to fundamentally different physical processes. The HBT coincidence count bump is *not* linked to stimulated emission—it occurs even if the input field is attenuated. Moreover, in the weak coupling approximation, any absorption or stimulated emission of the input pulse is negligibly small—the output field intensity is approximately equal to the sum of the input and atomic field intensities, considered as independent sources.

The same formalism can be used to model our experiment involving phase-matched emission from an ensemble of atoms, Fig. 1(b). The three-level atoms (ground state $|g\rangle = |5S_{1/2},\ F = 2,\ m_F = 2\rangle$, intermediate state $|e\rangle = |5P_{3/2}, F = 3, m_F = 3\rangle$, and Rydberg state $|r\rangle = |nS_{1/2}, m_J = 1/2\rangle$) are prepared in a phase-matched superposition of ground and Rydberg states using an excitation pulse of duration $T_E = 1\ \mu$s, consisting of two counterpropagating laser pulses E_1 and E_2 having central wavelengths 780 and 480 nm, respectively. Field E_1 drives the $|g\rangle \leftrightarrow |e\rangle$ transition with Rabi frequency Ω_1 and field E_2 drives the

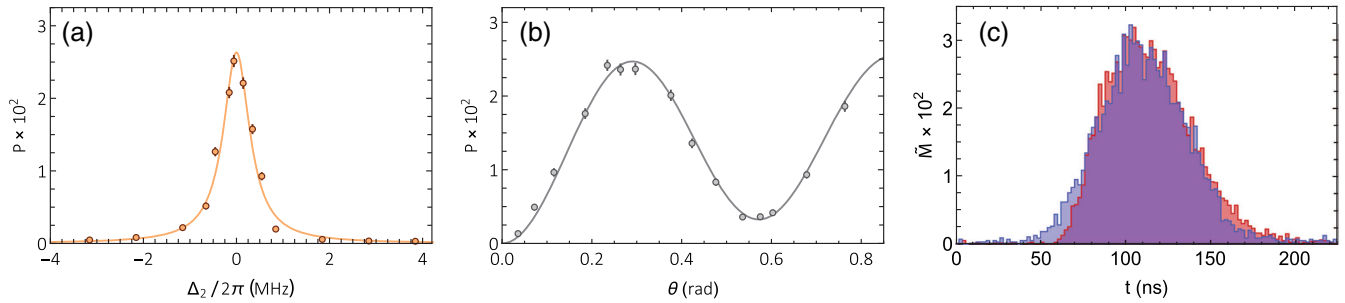

FIG. 2. Probing a collective (superatom) state. (a) Probability of photoelectric detection event per trial P as a function of two-photon detuning $\Delta_2 = \omega_{rg} - (\omega_{E_1} + \omega_{E_2})$ for the Rydberg state $|r\rangle = |87S_{1/2}\rangle$. The solid curve is a Lorentzian fit. The 0.8 MHz (FWHM) width of the peak is determined by the 1 μs excitation pulse duration. (b) P as a function of the collective Rabi angle θ displaying a period of a many-body (superatom) Rabi oscillation. The solid curve is a theory curve for a collective Rabi oscillation with $\Omega_2/2\pi = 1.5$ MHz and $\Omega_1/2\pi$ varied between 2 and 20 MHz. The best fit between theory and the data occurs for the number of atoms $N = 234$. (c) Normalized photocounts $\tilde{M}$ as a function of time t for the probe pulse (red) and the atomic emission (blue). The error bars represent $\pm$ one standard deviation ($\sqrt{M}$) for M photoelectric counting events.

$|e\rangle \leftrightarrow |r\rangle$ transition with Rabi frequency Ω_2. Field E_1 is detuned by an amount $\delta = -2\pi \times 90$ MHz from ω_{eg}. For a high-n Rydberg state [14], excitation of more than one atom into the Rydberg state can be suppressed, with the atomic ensemble being coherently driven between the collective ground state $|G\rangle$ and a singly excited (so-called superatom) collective state $|R\rangle$ at a frequency $\Omega_N = \sqrt{N}\Omega_1\Omega_2/(2\delta)$ [15–20]. After a delay $T_s \approx 0.5$ μs following the excitation pulse, a readout pulse E_R, centered at 480 nm is applied that is resonant with the $|r\rangle \leftrightarrow |e\rangle$ transition frequency and leads to phase-matched emission with $\omega_A = \omega_{eg}$.

Figure 2(a) displays the probability of photoelectric detection P as a function of two-photon detuning Δ_2 between $(\omega_{E_1} + \omega_{E_2})$ and ω_{rg}. The maximum probability of a photoelectric detection per trial is $P_{\max} \approx 2.5 \times 10^{-2}$ for a chosen value of $\theta \equiv \Omega_N T_E \simeq \pi$. Figure 2(b) shows P as a function of θ. Accounting for a factor of $\zeta = 0.27$ transmission and detection efficiency, there is a maximum probability $p_f \approx 0.09$ for a single photon to be emitted into the spatial mode defined by the single-mode fiber used for collection. A probe pulse whose temporal profile matches that of the phase-matched emission, and whose spatial mode corresponds to the detector acceptance mode, is also sent into the medium. In the absence of any Rydberg excitation, the transmission coefficient for the probe pulse is 0.45 ± 0.01. Figure 2(c) shows measured intensity profiles (normalized photocounts $\tilde{M}$ vs time t) for the probe pulse and the phase-matched atomic emission. The profiles are matched by adjusting both the readout and probe pulses, with their overlap integral being 0.94 for a 0.5 μs integration window and greater than 0.98 for a 0.1 μs integration window centered on their peak values. The value of the time-integrated second-order correlation function for atomic emission in the absence of the probe pulse is $g_A^{(2)} = 0.04$. The probe pulse can be delayed by a time τ relative to the phase-matched emission and the probe frequency ω_P can be detuned by an amount Δ from ω_A.

The total output field is sent into a beam splitter and detectors in the output mode of the beam splitter record coincidence counts. In the weak coupling approximation, any contribution to coincidence counts due to stimulated emission constitutes a small effect, of order $1/(Nk_0^2A) \simeq 10^{-6}$, where $k_0 = \omega_{21}/c$ and A is the cross-sectional area of the probe pulse. In fact, instead of being amplified by the medium, the output field intensity in the presence of Rydberg excitation is actually decreased by $\simeq 10^{-2}$.

The probe pulse is a weak, coherent state pulse having energy less than or of order $\hbar\omega_{eg}$. The atoms are prepared either into (1) a state consisting of a single phase-matched excitation by choosing an upper atomic state $|r\rangle = |87S_{1/2}\rangle$ with strong interactions [21–23], or (2) an upper atomic state $|r\rangle = |50S_{1/2}\rangle$, which leads to a factorized atomic state having on average $N_r \approx 1.5$ Rydberg excitations in the sample. In case (1), assuming that the spatial profiles of the probe and phase-matched emission pulses are identical, the number of photocounts separated in time by t_{21} is given by

$$N_c(t_{21}) = \int_{-\infty}^{\infty} dt \tilde{I}(t)\tilde{I}(t + t_{21})[1 + V_1(K)\cos(\Delta t_{21})], \tag{1}$$

where $\tilde{I}(t)$ is proportional to the intensity profile of the probe field, K is the ratio of integrated intensities for the input probe pulse and phase-matched emission, and $V_1(K) = 2K/(K^2 + 2K + g_A^{(2)})$ is the fringe visibility, allowing for a nonzero value of $g_A^{(2)}$. As was the case for a two-level atom, Eq. (1) is derived assuming that atom-field interactions are negligibly small, that is, no effects

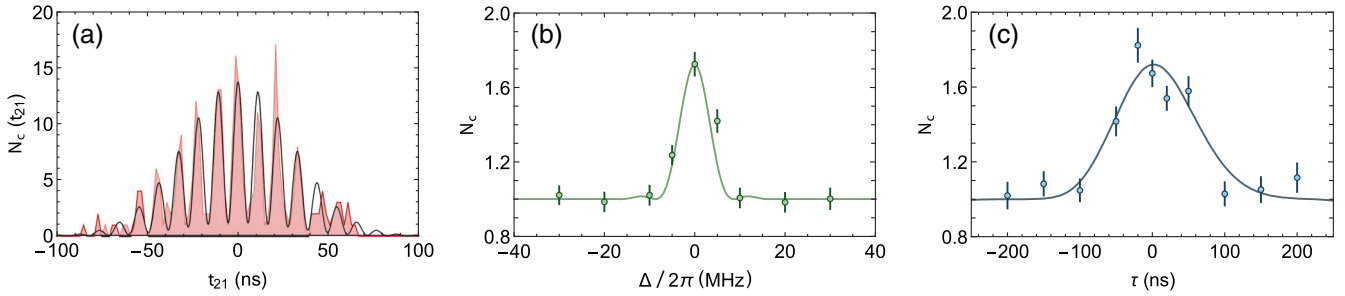

FIG. 3. Two-photon statistics for the upper atomic state $|r\rangle = |87S_{1/2}\rangle$. (a) Coincidences in a 2-ns window $N_c(t_{21})$ as a function of t_{21} for detuning $\Delta/2\pi = -80$ MHz between the probe field and the field emitted by the atoms. (b) Normalized integrated coincidences N_c as a function of the detuning Δ between the probe pulse and the pulse from the ensemble. (c) N_c as a function of the delay τ between the probe pulse and the pulse from the ensemble. Solid curves in (a)–(c) are obtained using our theoretical model.

related to stimulated emission are included. In Fig. 3(a), we plot measured values of $N_c(t_{21})$ for $K = 0.21$. The theory curve is obtained assuming a Gaussian profile for $\tilde{I}(t)$ and an expected value of $V_1(0.21) = 0.83$.

The normalized time-integrated coincidence counts are given by

$$N_c = 1 + 2K|J|^2/[K^2 + 2K + g_A^{(2)}], \tag{2}$$

where $J \equiv \int_{-\infty}^{\infty} e^{-i\Delta t} S(t-\tau) f(t) dt$ is an overlap integral of the two fields, and $S(t)$ and $f(t)$ are the (real) scaled amplitudes of the phase-matched and probe fields, respectively, normalized such that $\int_{-\infty}^{\infty} dt S^2(t) = 1$, $\int_{-\infty}^{\infty} dt f^2(t) = 1$. In this case, we allow for a slight difference between the intensity profiles of the probe field and atomic emission. If the intensity envelopes are identical and if $K \ll 1$ and $g_A^{(2)} \ll 1$, the time-integrated coincidence counts are doubled provided $\Delta = 0$ and $\tau = 0$, from the case where $|\Delta|/\gamma_e \gg 1$ or $\gamma_e \tau \gg 1$.

In Fig. 3(b), N_c is plotted as a function of Δ for $\tau = 0$ and N_c is plotted as a function of τ for $\Delta = 0$ in Fig. 3(c). Equation (2) is strictly valid only under an assumption of an optically thin medium in which the fraction of energy radiated by the atoms in the phase-matched direction $p_f \ll 1$. Including corrections of order $p_f \approx 0.06$, we estimate the value of $N_c \simeq 1 + 2(1 - p_f)K|J|^2/(K^2 + 2K + g_A^{(2)})$. In Figs. 3(b) and 3(c), the theoretical curves are drawn using $\{K = 0.46, |J(\Delta = 0)|^2 = 0.98\}$ $[N_c(\Delta = 0) = 1.72]$ and $\{K = 0.35, |J(\tau = 0)|^2 = 0.94\}$ $[N_c(\tau = 0) = 1.72]$, respectively.

When a Rydberg blockade is operative, the problem can be reduced to an effective two-level problem involving transitions between the Dicke state and the ground state. As such, it is possible to envision a situation in which there is total inversion of the system. Although the probe field can produce stimulated emission on the inverted system, the observed factor of 2 increase in coincidence counts is *not* a consequence of stimulated emission. Rather, it is an indication of both the nonclassical nature of the atomic Dicke state and HBT interference.

As further evidence of the fact that the increase in coincidence counts results from HBT interference and not stimulated emission, we next consider a factorized initial atomic state for which $g^{(2)} = 1$ and there is no inversion. Assuming that there is no temporal coherence between the input pulse and the phase-matched emission and that $f(t) = S(t)$, $N_c(t_{21})$ is given by

$$N_c(t_{21}) = \int_{-\infty}^{\infty} dt \tilde{I}(t)\tilde{I}(t + t_{21})[1 + V_2(K)\cos(\Delta t_{21})],$$

where $V_2(K) = 2K/(1 + K)^2$ is the fringe visibility. In Fig. 4(a), we plot values of $N_c(t_{21})$ for the Rydberg state $|r\rangle = |50S_{1/2}\rangle$ and with $K = 0.98$. The solid curve is theory, with fringe visibility $V_2(0.98) \approx 0.50$. The fringe

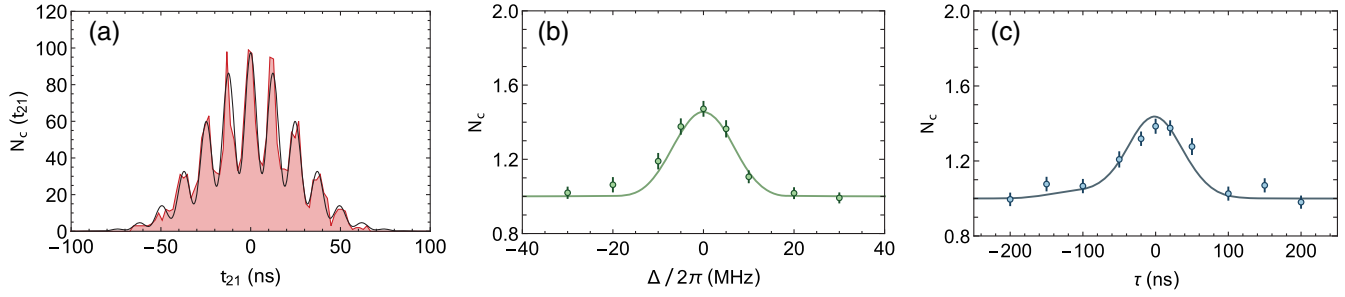

FIG. 4. Data and curves analogous to those shown in panels (a), (b), and (c) of Fig. 3, but for the upper atomic state $|r\rangle = |50S_{1/2}\rangle$.

visibility of $1/2$ is consistent with HBT interference between two coherent-state pulses, a situation that is mirrored by our choice of a factorized atomic state and a coherent-state probe pulse. For $K = 1$, the normalized time-integrated coincidence counts are given by $N_c = 1 + \frac{1}{2}|J|^2$. It is seen that, in this case, for $f(t) = S(t)$, the time-integrated coincidence rates are increased by a factor of $3/2$ provided $\Delta = 0$ and $\tau = 0$, from the case where $|\Delta|/\gamma_e \gg 1$ or $\gamma_e \tau \gg 1$. Figures 4(b) and 4(c) show N_c as a function of pulse detuning and delay, respectively, together with theory curves for which the enhancement factor $N_c \simeq 1 + 2(1 - p_f)|J|^2 K/(1 + K)^2$. In Figs. 4(b) and 4(c), the theoretical curves are drawn using $\{K = 0.90, |J(\Delta = 0)|^2 = 0.97\}$ $[N_c(\Delta = 0) = 1.46]$ and $\{K = 1.00, |J(\tau = 0)|^2 = 0.93\}$ $[N_c(\tau = 0) = 1.44]$, respectively. Again, although stimulated emission is negligible, there is an enhancement in coincidence counts when the probe pulse overlaps with the phase-matched atomic emission.

In conclusion, the interaction between the incident probe field with the atoms experiments such as ours and in Refs. [2–7] can be treated in a weak coupling approximation. In that limit, the increase in coincidence counts can be fully described by HBT-type interference between the incident field and the field radiated by the medium. There is no direct connection with stimulated emission.

This work was supported by the ARL Center for Distributed Quantum Information, Air Force Office of Scientific Research, and the National Science Foundation.

[1] A. Einstein, The quantum theory of radiation, Physikalische Zeitschrift **18**, 121 (1917).
[2] A. Lamas-Linares, J. C. Howell, and D. Bouwmeester, Stimulated emission of polarization-entangled photons, Nature (London) **412**, 887 (2001).
[3] A. Lamas-Linares, C. Simon, J. C. Howell, and D. Bouwmeester, Experimental quantum cloning of single photons, Science **296**, 712 (2002).
[4] F. W. Sun, B. H. Liu, Y. X. Gong, Y. F. Huang, Z.-Y. Ou, and G. C. Guo, Stimulated Emission as a Result of Multiphoton Interference, Phys. Rev. Lett. **99**, 043601 (2007).
[5] S. Dong, X. Yao, W. Zhang, S. Chen, W. Zhang, L. You, Z. Wang, and Y. F. Huang, True single-photon stimulated four-wave mixing, ACS Photonics **4**, 746 (2017).
[6] Z. Y. Ou, L. J. Wang, and L. Mandel, Photon amplification by parametric down-conversion, J. Opt. Soc. Am. B **7**, 211 (1990).
[7] Z. Y.-Ou, *Multi-Photon Quantum Interference* (Springer-Verlag, Berlin, 2007).
[8] R. H. Dicke, Coherence in spontaneous radiation processes, Phys. Rev. **93**, 99 (1954).
[9] P. R. Berman and A. Kuzmich, Coincidence counts and stimulated emission resulting from weak pulsed field—atomic interactions, Phys. Rev. A (to be published).
[10] R. Hanbury Brown and R. Q. Twiss, Correlation between photons in two coherent beams of light, Nature (London) **177**, 27 (1956).
[11] See Supplemental Material at http://link.aps.org/supplemental/10.1103/PhysRevLett.123.203603 for additional experimental and theoretical details, including an argument to support our claim that the increase in coincidence counts in down-conversion experiments can be attributed to HBT interference.
[12] P. R. Berman and V. S. Malinovsky, *Principles of Laser Spectroscopy and Quantum Optics* (Princeton University Press, Princeton, NJ, 2011).
[13] M. Cray, M.-L. Shih, and P. W. Milonni, Stimulated emission, absorption, and interference, Am. J. Phys. **50**, 1016 (1982).
[14] T. F. Gallagher, *Rydberg Atoms* (Cambridge University Press, Cambridge, England, 1994).
[15] E. Urban, T. A. Johnson, T. Henage, L. Isenhower, D. D. Yavuz, T. G. Walker, and M. Saffman, Observation of Rydberg blockade between two atoms, Nat. Phys. **5**, 110 (2009).
[16] A. Gaëtan, Y. Miroshnychenko, T. Wilk, A. Chotia, M. Viteau, D. Comparat, P. Pillet, A. Browaeys, and P. Grangier, Observation of collective excitation of two individual atoms in the Rydberg blockade regime, Nat. Phys. **5**, 115 (2009).
[17] Y. O. Dudin, L. Li, F. Bariani, and A. Kuzmich, Observation of coherent many-body Rabi oscillations, Nat. Phys. **8**, 790 (2012).
[18] M. Ebert, A. Gill, M. Gibbons, X. Zhang, M. Saffman, and T. G. Walker, Atomic Fock State Preparation Using Rydberg Blockade, Phys. Rev. Lett. **112**, 043602 (2014).
[19] D. Barredo, S. Ravets, H. Labuhn, L. Béguin, A. Vernier, F. Nogrette, T. Lahaye, and A. Browaeys, Demonstration of a Strong Rydberg Blockade in Three-Atom Systems with Anisotropic Interactions, Phys. Rev. Lett. **112**, 183002 (2014).
[20] J. Zeiher, P. Schauß, S. Hild, T. Macrì, I. Bloch, and C. Gross, Microscopic Characterization of Scalable Coherent Rydberg Superatoms, Phys. Rev. X **5**, 031015 (2015).
[21] Y. O. Dudin and A. Kuzmich, Strongly interacting Rydberg excitations of a cold atomic gas, Science **336**, 887 (2012).
[22] D. Maxwell, D. J. Szwer, D. Paredes-Barato, H. Busche, J. D. Pritchard, A. Gauguet, K. J. Weatherill, M. P. A. Jones, and C. S. Adams, Storage and Control of Optical Photons Using Rydberg Polaritons, Phys. Rev. Lett. **110**, 103001 (2013).
[23] L. Li, Y. O. Dudin, and A. Kuzmich, Entanglement between light and an optical atomic excitation, Nature (London) **498**, 466 (2013).